Oxygen isotope exchange between water and carbon dioxide in soils is controlled by pH, nitrate and microbial biomass through links to carbonic anhydrase activity

Sam P. Jones[1,3], Aurore Kaisermann[1], Jérôme Ogée[1], Steven Wohl[1], Alexander W. Cheesman[2], Lucas A. Cernusak[2] and Lisa Wingate[1]

[1] INRAE, UMR ISPA, 33140, Villenave d'Ornon, France
[2] College of Science and Engineering, James Cook University, Cairns, Queensland, Australia
[3] Instituto Nacional de Pesquisas da Amazônia, Manaus – AM, Brasil

Correspondence to: Sam P. Jones (sam.p.jones@hotmail.co.uk)

Abstract. The oxygen isotope composition of atmospheric carbon dioxide (CO_2) is intimately linked to large-scale variations in the cycling of CO_2 and water across the Earth's surface. Understanding the role the biosphere plays in modifying the oxygen isotope composition of atmospheric CO_2 is particularly important as this isotopic tracer has the potential to constrain estimates of important processes such as gross primary production at large-scales. However, constraining the atmospheric mass budget for the oxygen isotope composition of CO_2 also requires that we understand better the contribution of soil communities and how they influence the rate of oxygen isotope exchange between soil water and CO_2 (k_{iso}) across a wide range of soil types and climatic zones. As the carbonic anhydrases (CAs) group of enzymes enhances the rate of CO_2 hydration within the water-filled pore spaces of soils it is important to develop understanding of how environmental drivers can impact k_{iso} through changes in their activity. Here we estimate k_{iso} and measure associated soil properties in laboratory incubation experiments using 44 soils sampled from sites across western Eurasia and northeastern Australia. Observed values for k_{iso} always exceeded theoretically-derived uncatalysed rates, indicating a significant influence of CAs on the variability of k_{iso} across the soils studied. We identify soil pH as the principal source of variation, with greater k_{iso} under alkaline conditions suggesting that shifts in microbial community composition or intra-extra cellular dissolved inorganic carbon gradients induce the expression of more or higher activity forms of CAs. We also show for the first time in soils that the presence of nitrate under naturally acidic conditions reduces k_{iso}, potentially reflecting a direct or indirect inhibition of CAs. This effect appears to be supported by a supplementary ammonium nitrate fertilisation experiment conducted on a subset of the soils. Greater microbial biomass also increased k_{iso} under a given set of chemical conditions highlighting a putative link between CA expression and the abundance of soil microbes. These data provide the most extensive analysis of spatial variations in soil k_{iso} to date and indicate the key soil trait datasets required to predict variations in k_{iso} at large spatial scales, a necessary next step to constrain the important role of soil communities in the atmospheric mass budget of the oxygen isotope composition of CO_2.

1 Introduction

Quantifying the carbon storage potential of terrestrial ecosystems and its sensitivity to climate change relies on our ability to obtain observational constraints of photosynthesis and respiration at large scales (Beer et al., 2010). Over recent decades there has been increasing interest in using the oxygen isotope composition ($\delta^{18}O$ and $\delta^{17}O$) of atmospheric carbon dioxide (CO_2) to trace these large and opposing CO_2 fluxes. This is possible because the $\delta^{18}O$ of leaf-atmosphere CO_2 exchange is relatively enriched in ^{18}O compared to that of atmospheric CO_2 and the $\delta^{18}O$ of soil-atmosphere CO_2 exchange (Francey & Tans, 1987; Wingate et al., 2009; Welp et al., 2011). Similarly, photochemical processes in the stratosphere cause anomalies between the $\delta^{17}O$ and $\delta^{18}O$ of atmospheric CO_2 that are subsequently reset during leaf-atmosphere CO_2 exchange (Hoag et al., 2005; Koren et al., 2019; Adnew et al., 2020). However, the routine use of these tracers to constrain the photosynthetic term of the atmospheric mass budget for the $\delta^{18}O$ and $\delta^{17}O$ of CO_2 has been hampered by an incomplete understanding of how the influence of soil-atmosphere CO_2 exchange varies across different soil types and environmental conditions. Here we focus on $\delta^{18}O$ but the key challenges to understanding these variations are also relevant to considerations of $\delta^{17}O$.

Both soil respiration and leaf photosynthesis influence the $\delta^{18}O$ of atmospheric CO_2 because of the exchange of oxygen isotopes between water and CO_2 molecules during the reversible hydration of CO_2 to bicarbonate (Mills & Urey, 1940). In a closed system at chemical equilibrium, CO_2 will reach isotopic equilibrium with water after some time depending on the rate of this oxygen isotope exchange, k_{iso} (s^{-1}) (Uchikawa & Zeebe, 2012). Predicting variations in k_{iso} within soils is one of the key uncertainties in estimating the $\delta^{18}O$ of soil-atmosphere CO_2 exchange at large scales. As a consequence of this isotopic exchange, any CO_2 molecules invading soils from the atmosphere or being produced in the soil during respiration or organic matter decomposition will gradually inherit the $\delta^{18}O$ of the soil water pool as it diffuses within the soil profile (Tans, 1998). The degree to which the $\delta^{18}O$ of CO_2 inherits the $\delta^{18}O$ of a given soil water pool is determined by the residence time of dissolved CO_2 and the apparent k_{iso} (Miller et al., 1999). Longer residence times or greater k_{iso} move the system closer to isotopic equilibrium. As k_{iso} results from the interconversion of aqueous CO_2 and bicarbonate, k_{iso} is expected to vary as a function of the combined rates of CO_2 hydration, k_h, and hydroxylation reactions as well as the pH dependent speciation of dissolved inorganic carbon (DIC) (Uchikawa & Zeebe, 2012) (Fig. 1).

The rate of CO_2 hydration, k_h, is enhanced in the presence of enzymes known as carbonic anhydrases (CAs). Currently, at least seven distinct CA gene families have been identified, with each catalysing the reversible hydration of CO_2 to bicarbonate (Jensen et al., 2019). Whilst this reaction occurs abiotically (Fig. 1a), k_h is generally considered too slow for metabolic processes (Bar-Even et al., 2011; Merlin et al., 2003; Smith & Ferry, 2000). Consequently, the need for organisms

to rapidly control the transport and availability of CO_2, bicarbonate and protons in numerous metabolic pathways is considered the main driver underlying the convergent evolution of these enzymes (Smith & Ferry, 2000). Various lines of evidence indicate that a wide diversity of microbes carry the genes for multiple CAs (Smith et al., 1999) and that these genes are expressed in soils (Meredith et al., 2019). The presence of active CAs in soils, through the influence of enhanced k_h on k_{iso}, helps explain variations in the $\delta^{18}O$ of soil-atmosphere CO_2 exchange observed under field (Seibt et al., 2006; Wingate et al., 2008, 2009, 2010) and laboratory conditions (Jones et al., 2017; Meredith et al., 2019; Sauze et al., 2017, 2018). The size and composition of microbial communities present may thus be an important control on the apparent k_{iso} of soils (Wingate et al, 2009).

Soil pH strongly regulates the capacity of soils to store and supply nutrients and exerts control on the productivity of terrestrial ecosystems (Slessarev et al., 2016). It is well established that pH has a strong effect on the dominant forms of DIC (Fig. 1 b) and thus may influence the $\delta^{18}O$ of soil-atmosphere CO_2 exchange through its affect on k_{iso} (Fig. 1 c). Moreover, the combined impact of pH and DIC speciation leads to an optima, occuring under slightly acidic conditions, in the response of k_{iso} to increased rates of CO_2 hydration, k_h, in the presence of CAs (Fig. 1 c). Labratory experiments have shown that k_h, and consequently k_{iso} for different carbonic anhydrases (α-CA and β-CA for a given concentration and efficiency) are relatively lower under acidic conditions compared to the rates observed in neutral and slightly alkaline conditions (Rowlett et al., 2002; Sauze et al., 2018). Primarily, this behaviour is caused by the presence of high proton concentrations surrounding the enzyme at low pH values that leads to an inhibition of the de-protonation step required for enzyme regeneration (Rowlett et al., 2002). In contrast, k_{iso} decreases independently from k_h under alkaline conditions owing to a predominance of bicarbonate and carbonate ions and a correspondingly low abundance of CO_2 (Fig. 1 b; Uchikawa & Zeebe, 2021). Based on this knowledge of how k_{iso} varies with pH and DIC in the presence (and absence) of CA it seems probable that spatial variations in soil pH often found in different biomes will impact the apparent k_{iso} and $\delta^{18}O$ of soil-atmosphere CO_2 exchange.

Microbes, like most organisms must maintain a tightly regulated internal pH value of around 7 to ensure protein function and survive in a vast majority of soil environments (Hesse et al., 2002; Krulwich et al., 2011; Slonczewski et al., 2009). Carbonic anhydrases appear to play an important role in buffering organisms from potentially harmful changes in the pH (Slonczewski et al., 2009; Krulwich et al., 2011) and DIC levels of their surrounding environment (Smith & Ferry, 2000). For example, Krulwich et al. (2011) indicate that there may be an up-regulation of CA expression as certain microbes are moved from neutral to acidic pH conditions. Likewise, bacteria and fungi grown under CO_2 limited conditions can also up-regulate their CA expression (Amoroso et al., 2005; Kaur et al., 2009; Kozliak et al., 1995; Merlin et al., 2003). This suggests that the simple relationships with pH described in Fig. 1 for pure CAs in aqeuous solutions may not hold for soils where microbial communities may utilise both intra- and extra-cellular CAs and dynamically fine-tune CA expression in response to changes in the surrounding environment. Currently, very few datasets exist to be able to probe this caveat but it remains an

important challenge that must be resolved to understand large scale variations in apparent k_{iso} and the $\delta^{18}O$ of soil-atmosphere CO_2 exchange.

Various anions may also play a role in controlling the activity of CAs (Tibell et al., 1984). In particular, nitrate (NO_3^-) has been shown to inhibit different CAs in a range of microbes and plants (Amoroso et al., 2005; Innocenti et al., 2004; Peltier et al., 1995). This suggests that variations in soil nutrient availability between ecosystems could give rise to differences in k_{iso}. Furthermore, the addition of common fertilisers such as ammonium nitrate (NH_4NO_3) to agricultural soils could have an inhibitory role on CA activity in addition to causing shifts in the size and composition of microbial communities present Indeed, this hypothesis is supported by recent NH_4NO_3 fertilising experiments that demonstrated decreases in the CA catalysed hydrolysis of carbonyl sulphide (Kaisermann et al., 2018b). So far, the impact of nitrates on k_{iso} has not been investigated in soils.

Here we investigate variations in the rate of oxygen isotope exchange, k_{iso}, using controlled laboratory gas exchange measurements on soil incubations. To understand the drivers of these variations we measured soils, with different chemical and physical properties, sampled from 44 sites across western Eurasia and northeastern Australia. We also conducted a fertilisation experiment on a subset of these soils to investigate the influence of changes in nitrogen availability. Based on the potential controls on k_{iso} presented above we tested three specific, non-exclusive, hypotheses; 1) k_{iso} increases as microbial biomass increases (H1), 2) k_{iso} increases as soil pH increases (H2), and 3) k_{iso} decreases as the presence of NO_3^- increases (H3). For the Eurasian soils we also compare these drivers to the predictive power of relatively invariant soil properties that might be used to estimate the k_{iso} in soils at the regional scale and above as required by efforts to better constrain gross primary production.

2 Methods

To investigate the outlined hypotheses two similar measurement campaigns, each consisting of a spatial survey and an NH_4NO_3 addition experiment were conducted. These campaigns set out to characterise the variability and controls on the rate of oxygen isotope exchange, k_{iso}, across soils from a wide range of environments. In both cases we estimated k_{iso} from gas exchange and soil physical property measurements (Jones et al., 2017; Sauze et al., 2018). In addition, we measured the pH, microbial biomass, exchangeable NO_3^- and exchangeable NH_4^+ of the incubated soils to investigate the controls on k_{iso}. The first campaign focused on soils sampled from across western Eurasia (EUR) whilst the second (AUS) focused on soils sampled in north Queensland, Australia. Sampling sites were broadly classified using the principal land-cover reported by previous studies or observed during sampling and climatic zone as indicated by the Köppen-Geiger climate classification map of Kottek et al. (2006) and Rubel et al. (2017).

2.1 Soil sampling and incubation preparation

For the EUR campaign, the superficial 10 cm of soil was sampled at three locations within each of the 27 sites during the Northern hemisphere summer of 2016 (Fig. S1 a). These sites represented a range of forests (n = 16) and grasslands (n = 6) located in Subarctic (Dfc; n= 6), Temperate oceanic (Cfb; n= 13), Hot-summer Mediterranean (Csa; n = 7) and Hot semi-arid (Bsh; n = 1) climate zones. In addition we also sampled an agricultural field (n = 1), a peatland (n = 1) and some orchards (n = 3). Soil samples were transported at ambient temperatures to the Bordeaux- Nouvelle Aquitaine Center of the National Institute of Agricultural and Environmental Research (INRAE), France. Upon arrival, samples were passed through a 4 mm sieve and mixed to create one homogeneous sample for each site. These soils were stored at 4 °C. A sub-sample of each of these soils was used to determine the initial water content and the soil water holding capacity (Haney & Haney, 2010). For each soil three replicated incubations were prepared with glass jars of 15.54 cm in height and an internal diameter of 8.74 cm. Each jar was filled with the wet weight equivalent of 115 to 300 g of dry soil and the water content adjusted to 30 % of the water holding capacity to create a soil column with a surface area of 60.0 cm^2 and a depth of approximately 4 to 7 cm. The jars were then pre-incubated in a climate-controlled cabinet (MD1400, Snijders, Tilburg, NL) for two weeks in the dark at 22 ± 1 °C. This cabinet was continuously flushed with approximately 20 L min^{-1} of ambient air provided by a pump with an intake line outside the building to avoid exposing the soil to elevated CO_2 concentrations found within the laboratory. During this period, soil water content was periodically adjusted to account for evaporation. Approximately 18 hours prior to measurement the jar was closed with a screw-tight glass lid equipped with inlet and outlet connections and flushed at 250 mL min^{-1} with dry, synthetic air to promote steady-state conditions. This flow was produced using an in-house dilution system that mixed pure CO_2 from a cylinder into CO_2-free air generated by an air compressor (FM2 Atlas Copto, Nacka, Sweden) equipped with a scrubbing column (Ecodry K-MT6, Parker Hannifin, USA). This system was set to achieve a CO_2 concentration of 400 ± 5 ppm and, reflecting the origin of the CO_2 in the cylinder used, had a $\delta^{18}O$ of approximately −25 ‰ $VPDB_g$. Subsequently the jar was removed to conduct gas exchange and soil property measurements.

For the AUS campaign, we sampled the superficial 10 cm of soil at four locations within each of the 17 sites during July of 2017 and returned these samples on the same day to the Cairns campus of James Cook University (Fig. S1 b). These sites fell within Tropical monsoon (Am; n = 3), Humid subtropical (Cfa; n = 9) and Monsoon-influenced humid subtropical (Cwa; n= 5) climate zones and were principally found in forests (n = 9) and savannas (n = 6), with the other remaining sites located in a pasture (n = 1) and a stunted shrub-rich forest (n = 1). These soils were passed through a 4 mm sieve and mixed to create a homogenous sample for each site. A sub-sample of each of these soils was used to determine the initial water content and estimate the re-packed bulk density of the soils. As with the EUR campaign, three replicate incubations were prepared in glass jars for each soil. These jars had a height of 11.56 cm and an internal diameter of 7.45 cm. A jar was filled with the wet weight equivalent of 215 to 450 g of dry soil and the water content adjusted to 30 % water-filled pore space to create a soil column with a surface area of 43.5 cm^2 and a depth of approximately 8.5 cm. The jar was then pre-incubated in an insulated

box for one week in the dark at 23 ± 1 °C with periodic adjustments to the water content to account for evaporation. This box was continuously flushed with approximately 10 L min^{-1} of air provided by a compressor that serviced building wide laboratory air distribution. The concentration of CO_2 in this air was approximately 420 ppm and, and reflecting it's atmospheric origin, had a $\delta^{18}O$ of approximately 0 ‰ $VPDB_g$. Following pre-incubation the jar was removed to conduct gas exchange and soil property measurements.

An NH_4NO_3 addition experiment was also conducted in both campaigns. This involved the preparation of three additional replicated incubations as described above, for nine of the EUR sites and five of the AUS sites. Prior to the pre-incubation step, 0.7 mg of NH_4NO_3 g dry $soil^{-1}$ was dissolved in water and used to adjust the water content of these additional replicate incubations . These were then incubated alongside the three other 'control' incubations prepared as part of the spatial survery described above. The quantity of NH_4NO_3 applied was chosen to approximate a fertilisation treatment comparable to those typically applied in field studies (Ramirez et al., 2012).

2.2 Gas exchange measurements

Gas exchange measurements were made using a similar experimental set-up to that described in Jones et al. (2017). Each jar was connected to a gas delivery system that supplied one of two gas sources, $\delta_{b,atm}$ or $\delta_{b,mix}$, to its inlet. The first inlet condition, $\delta_{b,atm}$, consisted of a continuous flow of atmospheric air pumped from an external buffer volume, through a Drierite column (W. A. Hammond DRIERITE Co. LTD, USA) to dry the air and directly to the inlet of the jar. The second condition, $\delta_{b,mix}$, was produced by a second continuous flow of atmospheric air pumped from the buffer, through a soda lime column to remove CO_2 and a second Drierite column. A mass-flow controller was used to dilute pure CO_2 from a cylinder into this dry CO_2 free air and then this mix was supplied to the inlet of the jar. The flow rate of pure CO_2 was controlled to match the concentration of the CO_2 in $\delta_{b,mix}$ to that of $\delta_{b,atm}$ using a control loop feedback based on the difference in concentration between sub-samples of both flows measured with an infra-red CO_2 analyser (Li-6262, LI-COR Biosciences, USA). By doing so the principal difference between the two conditions was the isotopic composition of the CO_2 present reflecting its origin in the atmosphere ($\delta^{18}O$-CO_2 of $\delta_{b,atm}$ = −1.41 ± 2.17 ‰ $VPDB_g$) or a cylinder ($\delta^{18}O$-CO_2 of $\delta_{b,mix}$ = −25.33 ± 0.30 ‰ $VPDB_g$). Following this system the selected gas flow was split into a chamber line with a flow rate of 171.48 μmol s^{-1}, to which the jar was connected, and a bypass line that were measured by a CO_2 isotope ratio infrared spectrometer (Delta Ray IRIS, Thermo Fischer Scientific, Germany). The gas supply system sequentially supplied the two inlet conditions to these measurement lines. Both inlet conditions were supplied for either 32 (EUR) or 34 (AUS) minutes. The first 20 (EUR) or 22 (AUS) minutes under each condition were used to flush the system and promote steady-state conditions in the incubation jar. The turnover time of air in the jar was less than 10 minutes. After this period, the final 12 minutes during which the condition was supplied was used for gas-exchange measurements. During this period the IRIS measured the chamber and bypass lines three times each for two-minutes. Calibration gas was measured every 16 (EUR) or

18 (AUS) minutes with sequential two-minute measurements of two cylinders containing synthetic air with different CO_2 concentrations but similar isotopic compositions. The concentrations of $^{12}C^{16}O^{16}O$, $^{13}C^{16}O^{16}O$ and $^{12}C^{18}O^{16}O$ recorded by the IRIS were processed as described in detail by Jones et al. (2017) to average the final 40 s of data collected for each measurement and calculate corrected concentrations and isotope ratios. The associated precision for the total concentration and $\delta^{18}O$ of CO_2 was 0.02 ppm and 0.06 ‰ VPDBg respectively.

Reflecting the pre-incubation conditions, measurements for EUR began with $\delta_{b,mix}$ as the inlet condition before switching to $\delta_{b,atm}$, whilst for AUS the sequence began with $\delta_{b,atm}$ and then switched to $\delta_{b,mix}$. For EUR, the calibration cylinders (21 % O_2 and 0.93 % Ar in a N_2 balance, Deuste Steinger GmbH, Germany) had a total concentration, carbon isotope composition and $\delta^{18}O$ of CO_2, respectively, of 380.26 ppm , −3.06 ‰ VPDB, and −14.63 ‰ $VPDB_g$ for the first cylinder, and 481.62 ppm , −3.07 ‰ VPDB and 14.70 ‰ $VPDB_g$ for the second cylinder (IsoLab, Max Planck Institute for Biogeochemistry, Germany). For AUS, the calibration cylinders (21 % O_2 and 1.12 % Ar in a N_2 balance, BOC, Australia) had a total concentration, carbon isotope composition and $\delta^{18}O$ of CO_2, respectively, of 386.7 ppm, −33.42 ‰ VPDB and −26.33 ‰ $VPDB_g$, for the first cylinder, and 486.7 ppm, −33.64 ‰ VPDB and −26.60 ‰ $VPDB_g$ for the second cylinder (Farquhar Laboratory, Australian National University, Australia).

The net CO_2 flux, F_R (μmol m^{-2} s^{-1}), was calculated from corrected values for the three pairs of chamber and bypass line measurements made at each inlet condition following Eq. (1):

$$F_R = \frac{u}{A}\left(C_c - C_b\right), \quad (1)$$

where u is the flow rate (mol s^{-1}) through the chamber line, C_c is the total CO_2 concentration (ppm) of the chamber line, C_b is the total CO_2 concentration (ppm) of the bypass line and A is the surface area (m^2) of the soil in the chamber. The resultant three values for each inlet condition were then averaged to yield a single flux rate. Similarly the $\delta^{18}O$ of CO_2 exchange, δ_R (‰ $VPDB_g$), was calculated following Eq. (2):

$$\delta_R = \frac{\left(\delta_c C_{c,12} - \delta_b C_{b,12}\right)}{\left(C_{c,12} - C_{b,12}\right)}, \quad (2)$$

where δ_c is the $\delta^{18}O$ of CO_2 (‰ $VPDB_g$) in the chamber line, δ_b is the $\delta^{18}O$ of CO_2 (‰ $VPDB_g$) in the bypass line, $C_{c,12}$ (ppm) is the concentration of $^{12}C^{16}O^{16}O$ in the chamber line and $C_{b,12}$ (ppm) is the concentration of $^{12}C^{16}O^{16}O$ in the bypass line.

2.3 Soil properties

After being disconnected from the gas exchange system, a jar was weighed to determine the wet weight of the incubated soil and the total soil depth, z_{max} (m), measured using a caliper. Soil was then removed from the jar to determine soil water

content, pH, microbial biomass, exchangeable NO_3^- and exchangeable NH_4^+. Soil water contents were determined gravimetrically for sub-samples based on water loss after oven drying for 24 hours at 105 °C. In the EUR campaign, soil water content was determined for three, 1.5 cm thick intervals between 0 and 4.5 cm depth. An average gravimetric water content (g g dry soil^{-1}) was calculated for the soil column after weighting by total soil depth. In the AUS campaign, soil water content was determined for a single sample covering the total soil depth. Soil bulk density (g cm^{-3}) was calculated from the gravimetric water content, the wet weight of the soil in the jar and the volume of the soil column. Total porosity, ϕ_t, was calculated from bulk density assuming a particle density of 2.65 g cm^{-3} (Linn & Doran, 1984). Volumetric water content, θ_w (m^3 m^{-3}), was calculated as the product of gravimetric water content and bulk density. The soil air-filled porosity, ϕ_a, was calculated as the difference between the total porosity and volumetric water content. The remaining soil column in the jar was then mixed and sub-samples were taken to determine pH, microbial biomass, exchangeable NO_3^- and exchangeable NH_4^+. Soil pH was determined in a slurry with a dry weight equivalent soil-to-water ratio of 1:5. Soil microbial biomass (µg C g dry soil^{-1}) was determined based on the difference between dissolved carbon extracted from non-fumigated and chloroform-fumigated sub-samples using a slurry with a dry weight equivalent soil-to-potassium sulphate solution (0.5 M) ratio of 1:5 and an extraction efficiency value of 0.35. Exchangeable NO_3^- (µg N g dry soil^{-1}) and NH_4^+ (µg N g dry soil^{-1}) were extracted in a slurry with a dry weight equivalent soil-to-potassium chloride solution (1 M) ratio of 1:5. These extracts were filtered, frozen at −20 °C and shipped on dry ice to commercial laboratories (EUR: LAS INRAE Hauts-de-France, Arras, France; AUS: ASL Environmental, Brisbane, Queensland, Australia) for determination of dissolved carbon, NO_3^- and NH_4^+ concentrations. Sub-samples of the homogenised soil used to fill jars in the EUR campaign were also taken to determine soil texture and carbon and nitrogen content by sampling site as part of a related study (Kaisermann et al., 2018a).

2.4 Estimating the oxygen isotope exchange rate

Following Jones et al. (2017) the rate of oxygen isotope exchange between soil water and CO_2, k_{iso}, was estimated from the inverse of the slope of the linear relationship between the $\delta^{18}O$ of CO_2 exchange and the $\delta^{18}O$ of CO_2 at the soil surface. Briefly, under the two gas-exchange measurement conditions induced by varying the $\delta^{18}O$ of CO_2 at the incubation inlet ($\delta_{b,mix}$ and $\delta_{b,atm}$), the invasion flux or piston velocity of CO_2, v_{inv} (m s^{-1}), can be estimated following Eq. (3):

$$v_{\mathrm{inv}} = \frac{F_{\mathrm{R},\mu}}{C_{\mathrm{a},\mu}} \frac{\left(\delta_{\mathrm{R,mix}} - \delta_{\mathrm{R,atm}}\right)}{\left(\delta_{\mathrm{a,atm}} - \delta_{\mathrm{a,mix}}\right)} \quad , \tag{3}$$

where δ_R (‰ $VPDB_g$) is the $\delta^{18}O$ of CO_2 exchange and δ_a (‰ $VPDB_g$) is the $\delta^{18}O$ of CO_2 at the soil surface under the two different inlet conditions ($\delta_{b,mix}$ and $\delta_{b,atm}$) and $F_{R,\mu}$ (µmol m^{-2} s^{-1}) is the mean net CO_2 flux under both conditions and $C_{a,\mu}$ (µmol m^{-3}) is the mean total CO_2 concentration at the soil surface measured under both conditions. Both δ_a and C_a were assumed equal to the δ_c and C_c measured in the chamber line as discussed previously. To correct for the influence of

boundary conditions found at the bottom of incubation jars, particularly in shallower soil columns, the soil-depth adjusted invasion flux, $\tilde{v}_{inv}$ (m s^{-1}), was determined iteratively to satisfy Eq. (4):

$$0=\tilde{v}_{inv}\tanh\left(\frac{\tilde{v}_{inv}z_{max}}{\kappa\phi_a D}\right)-v_{inv} \quad , \tag{4}$$

where z_{max} (m) is the total soil-column depth, κ is soil tortuosity calculated here following the formulation of Moldrup et al. (2003) for repacked soils, D (m^2 s^{-1}) is the diffusivity of $^{12}C^{16}O^{18}O$ in air (Massman, 1998; Tans, 1998) and ϕ_a is the air-filled porosity of the soil (see Sauze et al., (2018) for the derivation). Subsequently k_{iso} (s^{-1}) was calculated following Eq. (5):

$$k_{iso}=\frac{\tilde{v}_{inv^2}}{\kappa\phi_a DB\theta_w} \quad , \tag{5}$$

where B (m^3 m^{-3}) is the Bunsen solubility coefficient for CO_2 in water (Weiss, 1974) and θ_w (m^3 m^{-3}) is the soil volumetric water content.

2.5 Statistical analyses

Statistical analyses were conducted in R version 3.5 (R Core Team, 2019). Of the 174 individual incubations prepared, 10 were excluded from the dataset because a record for one of the variables of interest; the rate, k_{iso}, of oxygen isotope exchange, pH, microbial biomass, exchangeable NO_3^- or exchangeable NH_4^+ was missing. For the remaining 164 incubations with complete records, these variables were averaged by sampling site and, for the relevant subset, by whether they received a NH_4NO_3 addition.

The resultant dataset consisted of mean observations for 44 untreated soils (n = 27 / EUR and 17 / AUS) and 14 soils (n = 9 / EUR and 5 / AUS) that received a NH_4NO_3 addition. Spatial controls on k_{iso} were investigated across the means of untreated soils. Correlations between k_{iso}, pH, microbial biomass, exchangeable NO_3^- and exchangeable NH_4^+ were investigated through the Spearman's rank correlation between pairs of variables. To test the outlined hypotheses, a multiple generalised linear modelling approach was used to investigate which variables best explained variations in k_{iso} (Thomas et al., 2017). As pH and exchangeable NH_4^+ were strongly negatively correlated (Spearman's $\rho = -0.73$) they were not considered together in the same model whilst all other possible combinations, including sampling campaign (EUR or AUS) to test for the undue influence of systematic experimental differences, were tested. Combinations were limited to models containing four or less predictive terms to prevent over-fitting and each independent variable was centered and scaled to facilitate comparison among the different measurement scales. The model structure and predictive terms included in the minimal adequate model required to explain variations in k_{iso} were selected based on a comparison of sample size corrected Aikake's Information

Criterion (AICc) and visual assessment of the conformity of model residuals to the assumptions of normality, homogeneity and the absence of unduly influential observations. This model was subsequently re-fitted with the original unstandardised variables. The same approach was also applied to the 27 soils from the EUR sampling campaign and extended to consider the relationships with soil texture and carbon and nitrogen contents to investigate their utility in up-scaling efforts. To prevent over-fitting, these models were limited to a maximum of two predictive terms. The predictive terms considered were soil sand, silt, clay, carbon and nitrogen content, the ratio of carbon to nitrogen content and soil pH.

To investigate the influence of the NH_4NO_3 addition on k_{iso}, the variables of interest were expressed as the ratio of the mean of the soils that received an addition and that of their respective untreated counterparts with quotients smaller and greater than one respectively indicating a reduction and increase following addition. Correlations between these fractional changes for k_{iso}, microbial biomass, pH, exchangeable NO_3^- and exchangeable NH_4^+ were investigated through the Spearman's rank correlation between pairs of variables. The minimal adequate, generalised linear model describing the fractional change in k_{iso} across these soils was investigated by comparing the AICc and visual inspection of the residuals for models that considered each independent variable separately to avoid over-fitting.

3 Results

3.1 Variations among untreated soils

Clear differences in k_{iso}, pH, microbial biomass, exchangeable NO_3^- and exchangeable NH_4^+ were not apparent as a function of sampling site climatic zone or land-cover (Fig. 2). Estimates of k_{iso} ranged from 0.01 to 0.40 s^{-1} with the greatest rates occurring in soils sampled from hot-summer Mediterranean (Csa), hot semi-arid (Bsh) and subtropical (Cfa and Cwa) climates (Fig. 2 a). Soil pH ranged from 3.9 to 8.6 and were mostly acidic or neutral with alkaline conditions only found for soils sampled from hot-summer Mediterranean (Csa) and hot semi-arid (Bsh) climates (Fig. 2 b). Ranging from 98.5 to 2898.1 µg C g dry $soil^{-1}$, microbial biomass did not appear to vary systematically with sampling site origin. Exchangeable NO_3^- ranged from 0.3 to 275.7 µg N g dry $soil^{-1}$ (Fig. 2 d) and exchangeable NH_4^+ ranged from 2.5 to 64.7 µg N g dry $soil^{-1}$ with greatest values found in soils sampled from temperate climates (Fig. 2 e).

Individual relationships between pairs of these variables were investigated through Spearman's rank correlation (Table 1). Strong, significant correlations ($p < 0.05$) were only found between k_{iso} and soil pH (Spearman's $\rho = 0.58$), k_{iso} and exchangeable NH_4^+ (Spearman's $\rho = -0.62$), and soil pH and exchangeable NH_4^+ (Spearman's $\rho = -0.73$). Correlations between all other variable pairings were weaker and non-significant ($p > 0.05$).

Based on AICc and visual inspection of model fit and residuals (Fig. S2), the structure of the generalised linear model describing variations in k_{iso} as the response variable was specified with a gaussian error distribution and log-link function (Thomas et al., 2017). The minimal adequate model with this structure included the additive effects of soil pH, the natural logarithm of exchangeable NO_3^-, the natural logarithm of microbial biomass, the interaction between soil pH and the natural logarithm of exchangeable NO_3^- and an intercept term (Fig. 3). This model explained 71 % of the deviance in k_{iso} (Fig. 4 a) compared to the null model containing only an intercept term. Its AICc was 6.1 lower than the next best alternative model that omitted the interaction term, 7.1 lower than the closest model containing sampling campaign and 13.3 lower than the closest model containing the natural logarithm of exchangeable NH_4^+ (Table S1). The AICc values of single-term models containing only pH or the natural logarithms of microbial biomass or exchangeable NO_3^- were respectively 21.6, 43.6, and 50.2 greater than the best model. The selected model predicts the response variable, $k_{iso\text{-}pred}$ (s^{-1}), in the original measurement units following Eq. (6):

$$\ln\left(k_{iso-pred}\right) = 0.122 \times pH - 0.730 \times \ln\left(NO_3^-\right) + 0.463 \times \ln\left(MB\right) + 0.109 \times pH \times \ln\left(NO_3^-\right) - 6.046 \quad , \quad (6)$$

where pH is soil pH, NO_3^- is exchangeable NO_3^- (µg N g dry $soil^{-1}$) and MB is microbial biomass (µg C g dry $soil^{-1}$). The model predicts that variations in k_{iso} result from positive correlations with soil pH (Fig. 3 a) and microbial biomass (Fig. 3 c) and negative correlation with exchangeable NO_3^-. The interaction between soil pH and exchangeable NO_3^- is such that the negative influence of NO_3^- on k_{iso} occurs mainly under acidic conditions and is marginal at neutral to alkaline pH (Fig. 3 b).

As with the full dataset, across the 27 soils from the EUR sampling campaign the strongest relationship describing k_{iso} was found with pH (Spearman's $\rho = 0.58$), whilst a weaker but still significant ($p < 0.05$) relationship with exchangeable NO_3^- (Spearman's $\rho = -0.42$) was also identified. No significant ($p > 0.05$) relationships between k_{iso} and clay (Spearman's $\rho = 0.11$), silt (Spearman's $\rho = -0.18$), sand (Spearman's $\rho = 0.00$), carbon (Spearman's $\rho = -0.03$) or nitrogen (Spearman's $\rho = -0.32$) contents were found, whilst, the relationship with the ratio of total carbon to nitrogen content (Spearman's $\rho = 0.38$) was marginal ($p = 0.05$). The minimal adequate generalised linear model (Table S2) explaining variations in k_{iso} selected from only the relatively invariant properties of soil texture and carbon and nitrogen content included only the intercept (−2.128) and the effect of nitrogen content (−0.119). This model explained 11 % of the deviance in k_{iso} compared to the null model. After inclusion of soil pH, the minimal adequate model included the intercept (−4.535) and the additive effects of soil pH (0.4028) and clay content (−0.0017). This model explained 61 % of the deviance in k_{iso} compared to 54 % for the model containing only the intercept (−4.535) and influence of soil pH (0.339).

3.2 Variations induced by NH_4NO_3 addition

The addition of NH_4NO_3 systematically increased exchangeable NO_3^- and NH_4^+ and decreased k_{iso} and soil pH. Exchangeable NO_3^- and NH_4^+ in the treated soils that received the NH_4NO_3 addition were respectively 1.9 to 173.6 and 3.7 to

18.8 times greater than in the corresponding untreated soils. Soil pH and k_{iso} were respectively 0.86 to 0.98 and 0.21 to 0.76 times smaller in the soils that received the addition compared with the corresponding untreated soils. The addition did not have a systematic influence on microbial biomass, which varied between 0.64 and 1.84 of the magnitude in the corresponding untreated soils. The absolute values of these changes are shown in Fig. S3.

Individual relationships between pairs of these fractional changes were investigated through Spearman's rank correlation (Table 2). Strong, significant correlations ($p < 0.05$) for variable pairs were found between the fractional changes in k_{iso} and soil pH (Spearman's $\rho = 0.57$), k_{iso} and exchangeable NO_3^- (Spearman's $\rho = -0.84$), and soil pH and exchangeable NO_3^- (Spearman's $\rho = -0.75$). Correlations between all other variable pairings were weaker and non-significant ($p > 0.05$).

Based on AICc and visual inspection of model fit and residuals, the structure of the generalised linear model describing variations in the fractional change in k_{iso} as the response variable was specified with a betareg error distribution and identity link function (Thomas et al., 2017). The minimal adequate, single term model with this structure included the natural logarithm of the fractional change in exchangeable NO_3^- (−0.499) and an intercept term (1.219). This model predicts the variations in the fractional change in k_{iso} following NH_4NO_3 addition across soils from the 14 sites considered result from a negative relationship with fractional changes in exchangeable NO_3^- (Fig. 5). This relationship explained 76 % of the deviance in the fractional change in k_{iso} and the model had an AICc that was 13.2 lower than the model that included the fractional change in soil pH and an intercept term (Table S3).

4 Discussion

This study aimed to reveal the drivers of variations in the oxygen isotope exchange rate, k_{iso}, to make it possible to predict the influence of different soil characteristics on the $\delta^{18}O$ of atmospheric CO_2 and improve our understanding of soil CA activity. To do so, controlled incubation experiments were conducted to estimate k_{iso} from soils collected across western Eurasia and northeastern Australia. Estimates of k_{iso} for untreated soils in this study ranged from 0.01 to 0.4 s^{-1} (Fig. 2 a). In all cases these rates exceeded theoretical uncatalysed rates (from 0.00008 to 0.008 s^{-1} depending on soil pH, Uchikawa & Zeebe, 2012), indicating the presence of active CAs. The median k_{iso} of 0.07 s^{-1} reported here is in the range of previously published values for sieved soils incubated in the dark (between 0.03 and 0.15 s^{-1}, Jones et al., 2017; Sauze et al., 2018, 2017) but lower than those reported by Meredith et al. (2019) with a median and range of 0.46 s^{-1} and 0.08 to 0.88 s^{-1}, respectively. These greater k_{iso} values reported by Meredith et al. (2019) are more comparable to values (between 0.01 to 0.75 s^{-1}) reported by Sauze et al. (2017) for soils with well-developed phototroph communities. Direct comparison of our estimates of k_{iso} with those observed in the field is challenging because these older studies (Seibt et al., 2006; Wingate et al., 2008, 2009, 2010) estimated soil CA activity as a range of enhancement factors over a temperature sensitive uncatalysed rate of hydration. However, using the mid-point of the enhancement factors and soil temperatures reported by Wingate et al.

(2009), we estimate that k_{iso} varied between 0.04 and 13 s^{-1} with a median of 0.31 s^{-1} across the seven ecosystems considered in their analysis. Understanding why k_{iso} can be orders of magnitude greater in the field compared to values observed in laboratory incubations is a key question for further studies. Potentially, the abundance and activity of CAs may be reduced during the process of sieving soils and incubating them for prolonged periods in the dark. For example, the exclusion of intact roots and mycorrhizal fungi interacting within the rhizosphere might reduce k_{iso} (Li et al., 2005). Equally the suppression of phototrophic community members by incubating soils in the dark (Sauze et al., 2017) may also contribute to differences in k_{iso} between the field and such experiments. Furthermore, we cannot exclude the possibility that determining k_{iso} accurately under field conditions is less reliable. For example, the calculation of k_{iso} relies on determining the $\delta^{18}O$ of the soil water pool in equilibrium with CO_2. Given the potential for increased heterogeneity in the soil water pool in natural conditions this may make it more challenging to determine k_{iso} robustly in the field (Jones et al., 2017).

At the outset of our study we hypothesised that k_{iso}, might be positively correlated with microbial biomass (H1), positively correlated with soil pH (H2) and negatively correlated with the presence of NO_3^- (H3). We found evidence in support of all three hypotheses, with the minimal adequate statistical model explaining variations in k_{iso} observed across untreated soils including all three of these terms (Eq. 6). The model suggests that the positive relationship with soil pH (Fig. 3 a), the strongest single predictor of variations in k_{iso}, reinforces the emergent view of soil pH as the principal driver of variations in CA expression in soil microbial communities (Sauze et al., 2018). The marked increases in k_{iso} observed for alkaline soils might reflect a shift in microbial community composition towards organisms that either express more CA protein as soil pH increases (higher 'community' concentrations) and/or express more efficient CAs than those found in acidic soils (Meredith et al., 2019; Sauze et al., 2018, 2017). Such putative mechanisms could be required to control the transport and availability of CO_2 and bicarbonate in response to the pH dependent speciation of DIC (Fig. 1 b) as previously observed for both intra- and extra-cellular CA activity in non-soil settings (Hopkinson et al., 2013; Kaur et al., 2009; Kozliak et al., 1995; Merlin et al., 2003). Similarly, the positive relationship found between k_{iso} and microbial biomass (Fig. 3 c) supports a secondary role, linking the abundance of microbes to the expression of CAs and k_{iso} for a given set of biogeochemical conditions (Wingate et al., 2009; Sauze et al., 2017). Finally, the negative relationship with exchangeable NO_3^- (Fig. 3 b) shows for the first time that k_{iso} in soils is sensitive to dissolved inorganic nitrogen chemistry. Anions including NO_3^- have previously been shown to inhibit CA activity by binding with the enzyme in non-soil systems (Amoroso et al., 2005; Peltier et al., 1995; Tibell et al., 1984). The fact that the binding and subsequent inhibition of CA activity has been shown to be more efficient under acidic conditions but have minimal influence at high pH may reflect the role of protonation in this behaviour (Johansson & Forsman, 1993, 1994). Interestingly, the larger negative influence of exchangeable NO_3^- in acidic soils identified here is in agreement with this observation (Fig. 3 b). This suggests that the influence of exchangeable NO_3^- on CA activity is reduced in neutral and alkaline soils and the constraints imposed by pH and microbial community size are of greater importance. To better understand the relationship between k_{iso} and soil inorganic nitrogen we conducted an NH_4NO_3 addition experiment. As

in other studies, the addition of NH_4NO_3 not only increased exchangeable NO_3^- and NH_4^+ but also decreased soil pH and caused non-systematic changes in microbial biomass (Fig. S3; Zhang et al., 2017). Reflecting the different magnitudes of these changes, the observed decrease in k_{iso} in soils receiving the addition relative to their untreated counterparts was best explained by the increase in exchangeable NO_3^- (Fig. 5). Notably the weak relationship between changes in k_{iso} and exchangeable NH_4^+ identified in this experiment (Table 2) suggests the relationship between these variables across the untreated soils (Table 1) does indeed reflect a co-correlation with soil pH rather than a direct causal link. The negative relationship between exchangeable NO_3^- and k_{iso} appears to support the proposed mechanism of CA inhibition. However, an alternative explanation, invoked to explain reductions in the activity of enzymes involved in nitrogen acquisition following fertilisation (Zhang et al., 2017), may be that CAs play some role in the soil nitrogen cycle that is alleviated by increases in exchangeable NO_3^- following NH_4NO_3 addition and thus leads to a down-regulation in CA expression (DiMario et al., 2017; Kalloniati et al., 2009; Rigobello-Masini et al., 2006). Indeed, such a function would help explain why the microbial communities in the untreated acidic, soils with higher exchangeable NO_3^- do not appear to need to compensate for the inhibition of CA. Such compensation might otherwise be expected from the economic theory of enzyme investment if CAs are facilitating important metabolic reactions (Burns et al., 2013). It is important to note that whilst the relationship between the changes in k_{iso} and exchangeable NO_3^- support observations from across the wider untreated dataset, the experimental design used in this addition experiment is not sufficient to fully test the influence of the combined changes in soil pH, exchangeable NO_3^-, exchangeable NH_4^+ and microbial biomass on k_{iso}. Further controlled, factorial experiments are required for this purpose. Further understanding of the intra- and extra-cellular distribution of microbial CAs and their relationship to spatial and temporal variations in soil chemical conditions are now required to confirm the mechanistic link among these observations.

Improvements in our ability to predict soil k_{iso} and its influence on the $\delta^{18}O$ of atmospheric CO_2 are important in refining the use of this tracer and others such as $\delta^{17}O$ to constrain photosynthesis and respiration at large scales (Wingate et al., 2009; Welp et al., 2011; Koren et al., 2020). Previous predictions of the $\delta^{18}O$ of soil-atmosphere CO_2 exchange were up-scaled using relationships observed in the field between k_{iso} and climate and/or land-cover (Wingate et al., 2009). In this study containing more measurements from a wider range of sites strong patterns with climate or land-cover were absent (Fig. 2 a). However, this could reflect the fact that the temperature and moisture conditions used in this study were unrepresentative of the field conditions especially for colder and drier sites. Our empirical model (Eq. 6) could provide broadly unbiased estimates of the observed variations in k_{iso} across the untreated soils of the 44 sites (Fig. 4 a). Indeed, the ability of this model to reasonably predict fractional changes in k_{iso} between untreated control soils, that were used to build the model, and their fertiliser treated counterparts, that were not used to 'train' the model selection process, is encouraging (Fig. 4 b). However, more observations from alkaline soils would be extremely useful to reduce the uncertainty found at greater k_{iso} (Fig. 3 a). A significant challenge to using this statistical relationship to predict k_{iso} is underpinned by our capacity to describe the spatial

and temporal variations in the important drivers of k_{iso}, namely soil pH, microbial biomass and exchangeable NO_3^-. For this reason we also considered whether more readily available parameters such as soil texture, carbon content and nitrogen content might provide an alternative basis for empirical predictions of k_{iso} (Van Looy et al., 2017). However, relationships between these variables and k_{iso} were relatively weak and could only explain a marginal amount of the observed variability. Fortunately, a number of promising spatial databases are evolving for soil characteristics such as pH and microbial biomass (Serna-Chavez et al., 2013; Slesserev et al., 2016). Likewise a number of land surface models can now estimate the spatial and temporal dynamics of the biosphere nitrogen cycle convincingly (Zaehle, 2013). Predictions of soil nutrient dynamics will likely depend on the use of such advanced soil nitrogen cycle models. Given the interaction between soil pH and exchangeable NO_3^- (Fig. 3 a & b), the absence of such data may not seriously compromise predictions for fertilised agricultural soils as typically they are not strongly acidic. However, accurately predicting natural spatial and seasonal variability and the influence of future changes in atmospheric NO_3^- deposition (DeForest et al., 2004) may be more problematic. Nonetheless, the data reported in this study now lay the foundations for an empirical approach to predicting k_{iso} for a wide range of soils using readily available maps of key soil traits. This represents an important breakthrough in predicting how variations in soil community CA activity impacts the $\delta^{18}O$ of atmospheric CO_2.

Data availability

The data produced in this study have been achived with PANGAEA (https://doi.org/10.1594/PANGAEA.928394). The data may also be requested from the corresponding author by email.

Competing interests

The authors declare that they have no conflict of interest.

Author contributions

Conceptualisation - SJ, AK, JO, SW, AC, LC & LW; Formal analysis – SJ & AK; Funding acquisition – JO & LW; Investigation – SJ, AK, SW, AC & LW; Methodology – SJ, AK, JO, SW & LW; Resources: JO, LC & LW; Writing (original draft) – SJ; Writing (review & editing) – SJ, JO, AC, LC & LW.

Acknowledgements

This work was funded by the European Research Council (ERC) under the European Union's Seventh Framework Programme (FP7/2007-2013) grant agreement No. 338264, and the Agence Nationale de la Recherche (ANR) grant number ANR-13-BS06-0005-01. Many thanks to Jorge Curiel-Yuste, Alexandria Correia, Jean-Marc Ourcival, Jukka Pumpanen, Huizhong Zhang, Carmen Emmel, Nina Buchmann, Sabina Keller, Irene Lehner, Anders Lindroth, Andreas Ibrom, Jens Schaarup Sorensen, Dan Yakir, Fulin Yang, Michal Heliasz, Susanne Burri, Penelope Serrano Ortiz, Maria Rosario Moya Jimenez, Jose Luis Vicente, Holger Tulp, Per Marklund, John Marshall, Nils Henriksson, Raquel Lobo de Vale, Lukas Siebicke, Bernard Longdoz, Pascal Courtois, and Katja Klumpp for providing soil from Eurasian sites, Joana Sauze, Ana Gutierrez, and Bastien Frejaville for facilitating analyses made in France, and Jon Lloyd, Camille Bathellier, Rolf Seigwolf, Matthias Saurer, Paul Nelson, Niels Munksgaard, Jen Whan, Michael Bird, Chris Wurster, and Hilary Stuart-Williams for facilitating analyses made in Australia.

References

Adnew, G. A., Pons, T. L., Koren, G., Peters, W. and Röckmann, T.: Leaf-scale quantification of the effect of photosynthetic gas exchange on $\Delta^{17}O$ of atmospheric CO_2, Biogeosciences, 17(14), 3903–3922, https://doi.org/10.5194/bg-17-3903-2020, 2020.

Amoroso, G., Morell-Avrahov, L., Müller, D., Klug, K. and Sültemeyer, D.: The gene NCE103 (YNL036w) from Saccharomyces cerevisiae encodes a functional carbonic anhydrase and its transcription is regulated by the concentration of inorganic carbon in the medium, Molecular Microbiology, 56(2), 549–558, https://doi.org/10.1111/j.1365-2958.2005.04560.x, 2005.

Bar-Even, A., Noor, E., Savir, Y., Liebermeister, W., Davidi, D., Tawfik, D. S. and Milo, R.: The Moderately Efficient Enzyme: Evolutionary and Physicochemical Trends Shaping Enzyme Parameters, Biochemistry, 50(21), 4402–4410, https://doi.org/10.1021/bi2002289, 2011.

Beer, C., Reichstein, M., Tomelleri, E., Ciais, P., Jung, M., Carvalhais, N., Rödenbeck, C., Arain, M. A., Baldocchi, D., Bonan, G. B., Bondeau, A., Cescatti, A., Lasslop, G., Lindroth, A., Lomas, M., Luyssaert, S., Margolis, H., Oleson, K. W., Roupsard, O., Veenendaal, E., Viovy, N., Williams, C., Woodward, F. I. and Papale, D.: Terrestrial Gross Carbon Dioxide Uptake: Global Distribution and Covariation with Climate, Science, 329(5993), 834–838, https://doi.org/10.1126/science.1184984, 2010.

Burns, R. G., DeForest, J. L., Marxsen, J., Sinsabaugh, R. L., Stromberger, M. E., Wallenstein, M. D., Weintraub, M. N. and Zoppini, A.: Soil enzymes in a changing environment: Current knowledge and future directions, Soil Biology and Biochemistry, 58, 216–234, doi:10.1016/j.soilbio.2012.11.009, 2013.

DeForest, J. L., Zak, D. R., Pregitzer, K. S. and Burton, A. J.: Atmospheric Nitrate Deposition, Microbial Community Composition, and Enzyme Activity in Northern Hardwood Forests, Soil Science Society of America Journal, 68(1), 132–138, doi:10.2136/sssaj2004.1320, 2004.

DiMario, R. J., Clayton, H., Mukherjee, A., Ludwig, M. and Moroney, J. V.: Plant Carbonic Anhydrases: Structures, Locations, Evolution, and Physiological Roles, Mol Plant, 10(1), 30–46, doi:10.1016/j.molp.2016.09.001, 2017.

Francey, R. J. and Tans, P. P.: Latitudinal variation in oxygen-18 of atmospheric CO2, Nature, 327(6122), 495–497, doi:10.1038/327495a0, 1987.

Haney, R. L. and Haney, E. B.: Simple and Rapid Laboratory Method for Rewetting Dry Soil for Incubations, Communications in Soil Science and Plant Analysis, 41(12), 1493–1501, doi:10.1080/00103624.2010.482171, 2010.

Hesse, S. J. A., Ruijter, G. J. G., Dijkema, C. and Visser, J.: Intracellular pH homeostasis in the filamentous fungus Aspergillus niger, European Journal of Biochemistry, 269(14), 3485–3494, https://doi.org/10.1046/j.1432-1033.2002.03042.x, 2002.

Hoag, K. J., Still, C. J., Fung, I. Y. and Boering, K. A.: Triple oxygen isotope composition of tropospheric carbon dioxide as a tracer of terrestrial gross carbon fluxes, Geophysical Research Letters, 32(2), https://doi.org/10.1029/2004GL021011, 2005.

Hopkinson, B. M., Meile, C. and Shen, C.: Quantification of Extracellular Carbonic Anhydrase Activity in Two Marine Diatoms and Investigation of Its Role, Plant Physiol., 162(2), 1142–1152, doi:10.1104/pp.113.217737, 2013.

Innocenti, A., Zimmerman, S., Ferry, J., Scozzafava, A. and Supuran, C.: Carbonic anhydrase inhibitors. Inhibition of the beta-class enzyme from the methanoarchaeon Methanobacterium thermoautotrophicum (Cab) with anions, Bioorganic & Medicinal Chemistry Letters, 14(17), 4563–4567, https://doi.org/10.1016/j.bmcl.2004.06.073, 2004.

Jensen, E. L., Clement, R., Kosta, A., Maberly, S. C. and Gontero, B.: A new widespread subclass of carbonic anhydrase in marine phytoplankton, The ISME Journal, 13(8), 2094–2106, doi:10.1038/s41396-019-0426-8, 2019.

Johansson, I.-M. and Forsman, C.: Kinetic studies of pea carbonic anhydrase, European Journal of Biochemistry, 218(2), 439–446, doi:10.1111/j.1432-1033.1993.tb18394.x, 1993.

Johansson, I.-M. and Forsman, C.: Solvent Hydrogen Isotope Effects and Anion Inhibition of CO2 Hydration Catalysed by Carbonic Anhydrase from Pisum sativum, European Journal of Biochemistry, 224(3), 901–907, doi:10.1111/j.1432-1033.1994.00901.x, 1994.

Jones, S. P., Ogée, J., Sauze, J., Wohl, S., Saavedra, N., Fernández-Prado, N., Maire, J., Launois, T., Bosc, A. and Wingate, L.: Non-destructive estimates of soil carbonic anhydrase activity and associated soil water oxygen isotope composition, Hydrology and Earth System Sciences, 21(12), 6363–6377, doi:https://doi.org/10.5194/hess-21-6363-2017, 2017.

Kaisermann, A., Ogée, J., Sauze, J., Wohl, S., Jones, S. P., Gutierrez, A. and Wingate, L.: Disentangling the rates of carbonyl sulfide (COS) production and consumption and their dependency on soil properties across biomes and land use types, Atmospheric Chemistry and Physics, 18(13), 9425–9440, doi:https://doi.org/10.5194/acp-18-9425-2018, 2018a.

Kaisermann, A., Jones, S. P., Wohl, S., Ogée, J. and Wingate, L.: Nitrogen Fertilization Reduces the Capacity of Soils to Take up Atmospheric Carbonyl Sulphide, Soil Systems, 2(4), 62, doi:10.3390/soilsystems2040062, 2018b.

Kalloniati, C., Tsikou, D., Lampiri, V., Fotelli, M. N., Rennenberg, H., Chatzipavlidis, I., Fasseas, C., Katinakis, P. and Flemetakis, E.: Characterization of a Mesorhizobium loti α-Type Carbonic Anhydrase and Its Role in Symbiotic Nitrogen Fixation, Journal of Bacteriology, 191(8), 2593–2600, doi:10.1128/JB.01456-08, 2009.

Kaur, S., Mishra, M. N. and Tripathi, A. K.: Regulation of expression and biochemical characterization of a β-class carbonic anhydrase from the plant growth-promoting rhizobacterium, Azospirillum brasilense Sp7, FEMS Microbiology Letters, 299(2), 149–158, doi:10.1111/j.1574-6968.2009.01736.x, 2009.

Koren, G., Schneider, L., Velde, I. R. van der, Schaik, E. van, Gromov, S. S., Adnew, G. A., Martino, D. J. M., Hofmann, M. E. G., Liang, M.-C., Mahata, S., Bergamaschi, P., Laan-Luijkx, I. T. van der, Krol, M. C., Röckmann, T. and Peters, W.: Global 3-D Simulations of the Triple Oxygen Isotope Signature Δ17O in Atmospheric CO2, Journal of Geophysical Research: Atmospheres, 124(15), 8808–8836, https://doi.org/10.1029/2019JD030387, 2019.

Kottek, M., Grieser, J., Beck, C., Rudolf, B. and Rubel, F.: World Map of the Köppen-Geiger climate classification updated, metz, 15(3), 259–263, doi:10.1127/0941-2948/2006/0130, 2006.

Kozliak, E. I., Fuchs, J. A., Guilloton, M. B. and Anderson, P. M.: Role of bicarbonate/CO2 in the inhibition of Escherichia coli growth by cyanate., J. Bacteriol., 177(11), 3213–3219, doi:10.1128/jb.177.11.3213-3219.1995, 1995.

Krulwich, T. A., Sachs, G. and Padan, E.: Molecular aspects of bacterial pH sensing and homeostasis, Nature Reviews Microbiology, 9(5), 330, doi:10.1038/nrmicro2549, 2011.

Li, W., Yu, L., Yuan, D., Wu, Y. and Zeng, X.: A study of the activity and ecological significance of carbonic anhydrase from soil and its microbes from different karst ecosystems of Southwest China, Plant Soil, 272(1–2), 133–141, doi:10.1007/s11104-004-4335-9, 2005.

Linn, D. M. and Doran, J. W.: Effect of Water-Filled Pore Space on Carbon Dioxide and Nitrous Oxide Production in Tilled and Nontilled Soils, Soil Science Society of America Journal, 48(6), 1267–1272, doi:10.2136/sssaj1984.03615995004800060013x, 1984.

Massman, W. J.: A review of the molecular diffusivities of H2O, CO2, CH4, CO, O3, SO2, NH3, N2O, NO, and NO2 in air, O2 and N2 near STP, Atmospheric Environment, 32(6), 1111–1127, doi:10.1016/S1352-2310(97)00391-9, 1998.

Meredith, L. K., Ogée, J., Boye, K., Singer, E., Wingate, L., Sperber, C. von, Sengupta, A., Whelan, M., Pang, E., Keiluweit, M., Brüggemann, N., Berry, J. A. and Welander, P. V.: Soil exchange rates of COS and CO 18 O differ with the diversity of microbial communities and their carbonic anhydrase enzymes, The ISME Journal, 13(2), 290, doi:10.1038/s41396-018-0270-2, 2019.

Merlin, C., Masters, M., McAteer, S. and Coulson, A.: Why Is Carbonic Anhydrase Essential to Escherichia coli?, J. Bacteriol., 185(21), 6415–6424, doi:10.1128/JB.185.21.6415-6424.2003, 2003.

Miller, J. B., Yakir, D., White, J. W. C. and Tans, P. P.: Measurement of 18O/16O in the soil-atmosphere CO2 flux, Global Biogeochem. Cycles, 13(3), 761–774, doi:10.1029/1999GB900028, 1999.

Mills, G. A. and Urey, H. C.: The Kinetics of Isotopic Exchange between Carbon Dioxide, Bicarbonate Ion, Carbonate Ion and Water1, J. Am. Chem. Soc., 62(5), 1019–1026, doi:10.1021/ja01862a010, 1940.

Moldrup, P., Olesen, T., Komatsu, T., Yoshikawa, S., Schjønning, P. and Rolston, D.: Modeling diffusion and reaction in soils: X. A unifying model for solute and gas diffusivity in unsaturated soil, Soil Science, 168(5), 321–337, 2003.

Peltier, G., Cournac, L., Despax, V., Dimon, B., Fina, L., Genty, B. and Rumeau, D.: Carbonic anhydrase activity in leaves as measured in vivo by<Superscript>18</Superscript>O exchange between carbon dioxide and water, Planta, 196(4), 732–739, doi:10.1007/BF01106768, 1995.

R Core Team: R: A Language and Environment for Statistical Computing, R Foundation for Statistical Computing, Vienna, Austria. [online] Available from: https://www.R-project.org/, 2019.

Ramirez, K. S., Craine, J. M. and Fierer, N.: Consistent effects of nitrogen amendments on soil microbial communities and processes across biomes, Global Change Biology, 18(6), 1918–1927, doi:10.1111/j.1365-2486.2012.02639.x, 2012.

Rigobello-Masini, M., Masini, J. C. and Aidar, E.: The profiles of nitrate reductase and carbonic anhydrase activity in batch cultivation of the marine microalgae Tetraselmis gracilis growing under different aeration conditions, FEMS Microbiology Ecology, 57(1), 18–25, doi:10.1111/j.1574-6941.2006.00106.x, 2006.

Rowlett, R. S., Tu, C., McKay, M. M., Preiss, J. R., Loomis, R. J., Hicks, K. A., Marchione, R. J., Strong, J. A., Donovan Jr., G. S. and Chamberlin, J. E.: Kinetic characterization of wild-type and proton transfer-impaired variants of β-carbonic anhydrase from Arabidopsis thaliana, Archives of Biochemistry and Biophysics, 404(2), 197–209, doi:10.1016/S0003-9861(02)00243-6, 2002.

Rubel, F., Brugger, K., Haslinger, K. and Auer, I.: The climate of the European Alps: Shift of very high resolution Köppen-Geiger climate zones 1800–2100, metz, 26(2), 115–125, doi:10.1127/metz/2016/0816, 2017.

Sauze, J., Ogée, J., Maron, P.-A., Crouzet, O., Nowak, V., Wohl, S., Kaisermann, A., Jones, S. P. and Wingate, L.: The interaction of soil phototrophs and fungi with pH and their impact on soil CO2, CO18O and OCS exchange, Soil Biology and Biochemistry, 115(Supplement C), 371–382, doi:10.1016/j.soilbio.2017.09.009, 2017.

Sauze, J., Jones, S. P., Wingate, L., Wohl, S. and Ogée, J.: The role of soil pH on soil carbonic anhydrase activity, Biogeosciences, 15(2), 597–612, doi:10.5194/bg-15-597-2018, 2018.

Seibt, U., Wingate, L., Lloyd, J. and Berry, J. A.: Diurnally variable δ18O signatures of soil CO2 fluxes indicate carbonic anhydrase activity in a forest soil, J. Geophys. Res., 111(G4), G04005, doi:10.1029/2006JG000177, 2006.

Serna-Chavez, H. M., Fierer, N. and Bodegom, P. M. van: Global drivers and patterns of microbial abundance in soil, Global Ecology and Biogeography, 22(10), 1162–1172, https://doi.org/10.1111/geb.12070, 2013.

Slonczewski, J. L., Fujisawa, M., Dopson, M. and Krulwich, T. A.: Cytoplasmic pH Measurement and Homeostasis in Bacteria and Archaea, in Advances in Microbial Physiology, vol. 55, edited by R. K. Poole, pp. 1–317, Academic Press, https://doi.org/10.1016/S0065-2911(09)05501-5, , 2009.

Smith, K. S., Jakubzick, C., Whittam, T. S. and Ferry, J. G.: Carbonic anhydrase is an ancient enzyme widespread in prokaryotes, PNAS, 96(26), 15184–15189, https://doi.org/10.1073/pnas.96.26.15184, 1999.

Smith, K. S. and Ferry, J. G.: Prokaryotic carbonic anhydrases, FEMS Microbiology Reviews, 24(4), 335–366, doi:10.1111/j.1574-6976.2000.tb00546.x, 2000.

Tans, P. P.: Oxygen isotopic equilibrium between carbon dioxide and water in soils, Tellus B, 50(2), doi:10.3402/tellusb.v50i2.16094, 1998.

Thomas, R., Lello, J., Medeiros, R., Pollard, A., Robinson, P., Seward, A., Smith, J., Vafidis, J. and Vaughan, I.: Data Analysis with R Statistical Software: A guidebook for Scientists, Eco-explore, Caerphilly, Wales., 2017.

Tibell, L., Forsman, C., Simonsson, I. and Lindskog, S.: Anion Inhibition of CO2 hydration catalyzed by human carbonic anhydrase II: Mechanistic implications, Biochimica et Biophysica Acta (BBA) - Protein Structure and Molecular Enzymology, 789(3), 302–310, doi:10.1016/0167-4838(84)90186-9, 1984.

Uchikawa, J. and Zeebe, R. E.: The effect of carbonic anhydrase on the kinetics and equilibrium of the oxygen isotope exchange in the CO2–H2O system: Implications for δ18O vital effects in biogenic carbonates, Geochimica et Cosmochimica Acta, 95, 15–34, doi:10.1016/j.gca.2012.07.022, 2012.

Van Looy, K., Bouma, J., Herbst, M., Koestel, J., Minasny, B., Mishra, U., Montzka, C., Nemes, A., Pachepsky, Y. A., Padarian, J., Schaap, M. G., Tóth, B., Verhoef, A., Vanderborght, J., Ploeg, M. J. van der, Weihermüller, L., Zacharias, S., Zhang, Y. and Vereecken, H.: Pedotransfer Functions in Earth System Science: Challenges and Perspectives, Reviews of Geophysics, 55(4), 1199–1256, doi:10.1002/2017RG000581, 2017.

Weiss, R. F.: Carbon dioxide in water and seawater: the solubility of a non-ideal gas, Marine Chemistry, 2(3), 203–215, doi:10.1016/0304-4203(74)90015-2, 1974.

Wingate, L., Seibt, U., Maseyk, K., Ogée, J., Almeida, P., Yakir, D., Pereira, J. S. and Mencuccini, M.: Evaporation and carbonic anhydrase activity recorded in oxygen isotope signatures of net CO2 fluxes from a Mediterranean soil, Global Change Biology, 14(9), 2178–2193, doi:10.1111/j.1365-2486.2008.01635.x, 2008.

Wingate, L., Ogée, J., Cuntz, M., Genty, B., Reiter, I., Seibt, U., Yakir, D., Maseyk, K., Pendall, E. G., Barbour, M. M., Mortazavi, B., Burlett, R., Peylin, P., Miller, J., Mencuccini, M., Shim, J. H., Hunt, J. and Grace, J.: The impact of soil microorganisms on the global budget of δ18O in atmospheric CO2, PNAS, 106(52), 22411–22415, doi:10.1073/pnas.0905210106, 2009.

Wingate, L., Ogée, J., Burlett, R. and Bosc, A.: Strong seasonal disequilibrium measured between the oxygen isotope signals of leaf and soil CO2 exchange, Global Change Biology, 16(11), 3048–3064, doi:10.1111/j.1365-2486.2010.02186.x, 2010.

Zaehle, S.: Terrestrial nitrogen–carbon cycle interactions at the global scale, Philosophical Transactions of the Royal Society B: Biological Sciences, 368(1621), 20130125, https://doi.org/10.1098/rstb.2013.0125, 2013.

Zhang, C., Zhang, X.-Y., Zou, H.-T., Kou, L., Yang, Y., Wen, X.-F., Li, S.-G., Wang, H.-M. and Sun, X.-M.: Contrasting effects of ammonium and nitrate additions on the biomass of soil microbial communities and enzyme activities in subtropical China, Biogeosciences, 14(20), 4815–4827, doi:https://doi.org/10.5194/bg-14-4815-2017, 2017.

Tables

Table 1: Spearman's rank correlation coefficients (ρ) for relationships between site mean oxygen isotope exchange rate (k_{iso}), soil pH, microbial biomass (MB), NO_3^- availability and NH_4^+ availability measured in untreated soils (n = 44). * indicates $p < 0.05$ and ** indicates $p < 0.01$.

	k_{iso}	pH	MB	NO_3^-	NH_4^+
k_{iso}	-	0.58**	0.16	−0.25	−0.62**
pH	0.58**	-	−0.27	0.01	−0.73**
MB	0.16	−0.27	-	0.29	0.05
NO_3−	−0.25	0.01	0.29	-	0.11
NH_4^+	−0.62**	−0.73**	0.05	0.11	-

Table 2: Spearman's rank correlation coefficients (ρ) for relationships between changes in the ratio of mean rate of oxygen isotope exchange (k_{iso}), soil pH, microbial biomass (MB), NO_3^- availability and NH4+ availability between soils receiving a NH_4NO_3 addition and that of the corresponding untreated soils (n = 14). * indicates $p < 0.05$ and ** indicates $p < 0.01$.

	k_{iso}	pH	MB	NO_3^-	NH_4^+
k_{iso}	-	0.57*	0.37	−0.84**	0.14
pH	0.57*	-	0.22	−0.75**	0.02
MB	0.37	0.22	-	−0.32	0.18
NO_3−	−0.84**	−0.75**	−0.32	-	0.09
NH_4^+	0.14	0.02	0.18	0.09	-

Figures

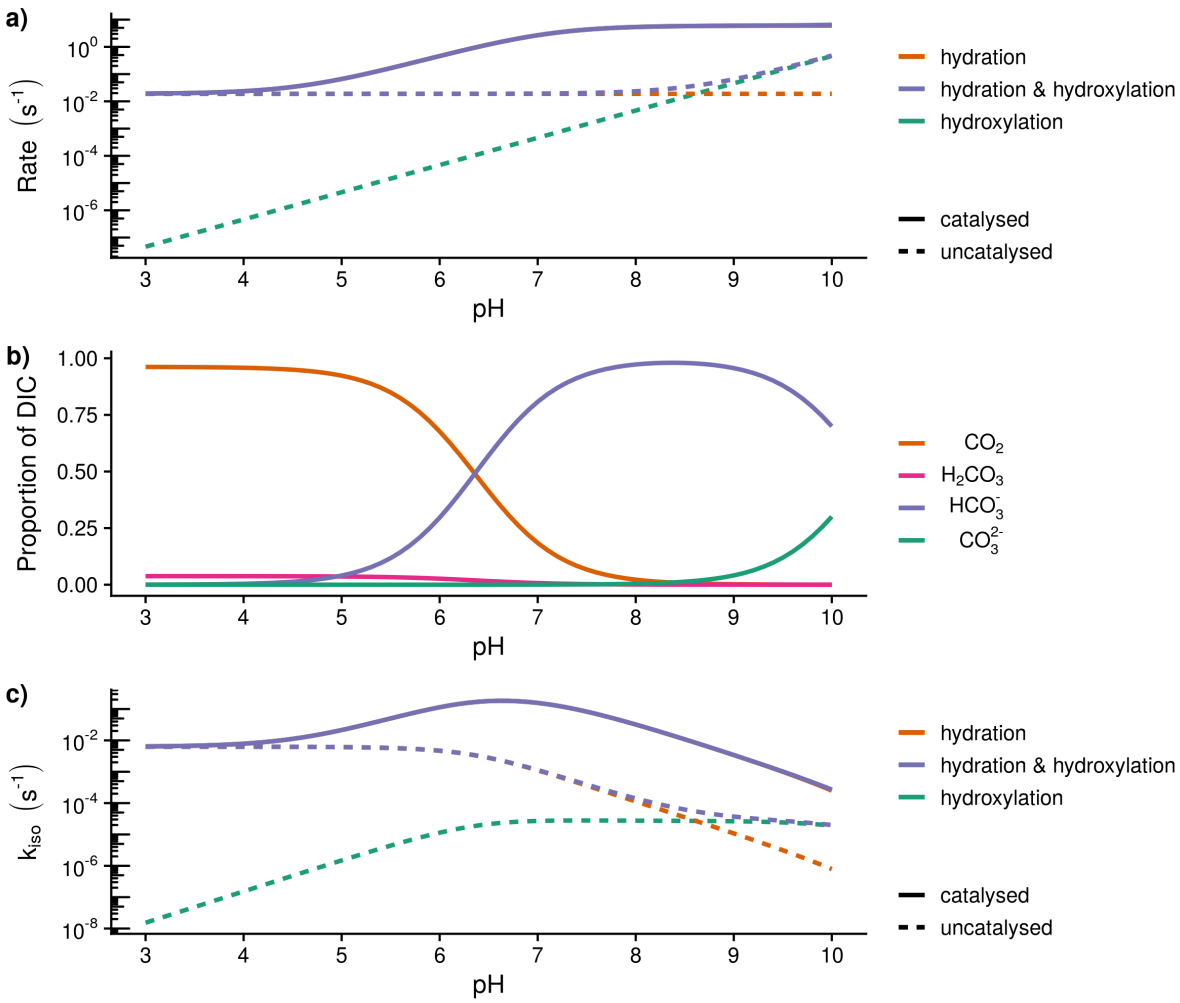

Figure 1: Theoretical calculations of the expected relationship between the rate of hydration (k_h) and hydroxylation reactions, the speciation of dissolved inorganic carbon (DIC) and the rate of oxygen isotope exchange (k_{iso}): a) expected variations in the rate of hydration (k_h) and hydroxylation reactions with pH at 21 °C calculated following Uchikawa & Zeebe (2012) and Sauze et al. (2018). Dashed lines indicate uncatalysed rates whilst solid lines include the presence of 200 nM of carbonic anhyrdrase with a $k_{cat}/k_m = 3 \times 10^7$ M s^{-1} and a pka of 7.1. The catalysed rate of hydration decreases under acidic conditions as high proton concentrations limit enzyme regeneration, b) Speciation of dissolved inorganic carbon (DIC) calculated from rate constants at 21 °C, c) Expected variations in the rate of isotope exchange (k_{iso}) with pH calculated as in the first panel (a). The rate of exchange is limited by enzyme regeneration under acidic conditions and the availability of CO_2 under alkaline conditions.

710

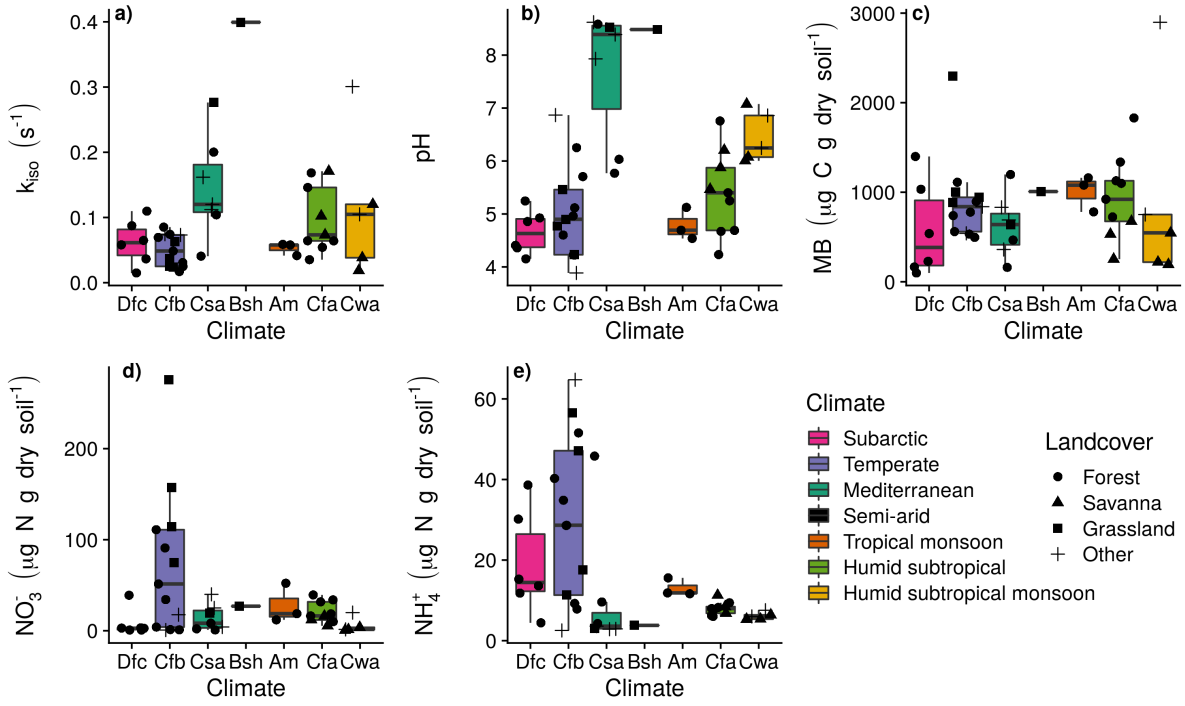

Figure 2: Measurement summaries of mean untreated soils by Köppen-Geiger climatic zone of the sampling site. The 27 sites in western Eurasian (EUR) were within Subartctic (Dfc; n= 6), Temperate oceanic (Cfb; n= 13), Hot-summer Mediterraean (Csa; n = 7) and Hot semi-arid (Bsh; n = 1) climate zones and the 17 sites in north Queensland, Australia (AUS) were within Tropical monsoon (Am; n = 3), Humid subtropical (Cfa; n = 9) and Monsoon-influenced humid subtropical (Cwa; n= 5) climate zones. Box lower, middle and upper hinges respectively indicate 0.25, 0.5 and 0.75 quantiles. Over-plotted points are the associated site means (n=2 or 3) with shape indicating land-cover: a) k_{iso}, b) pH, c) microbial biomass (MB), d) NO_3^- availability, and d) NH_4^+ availability.

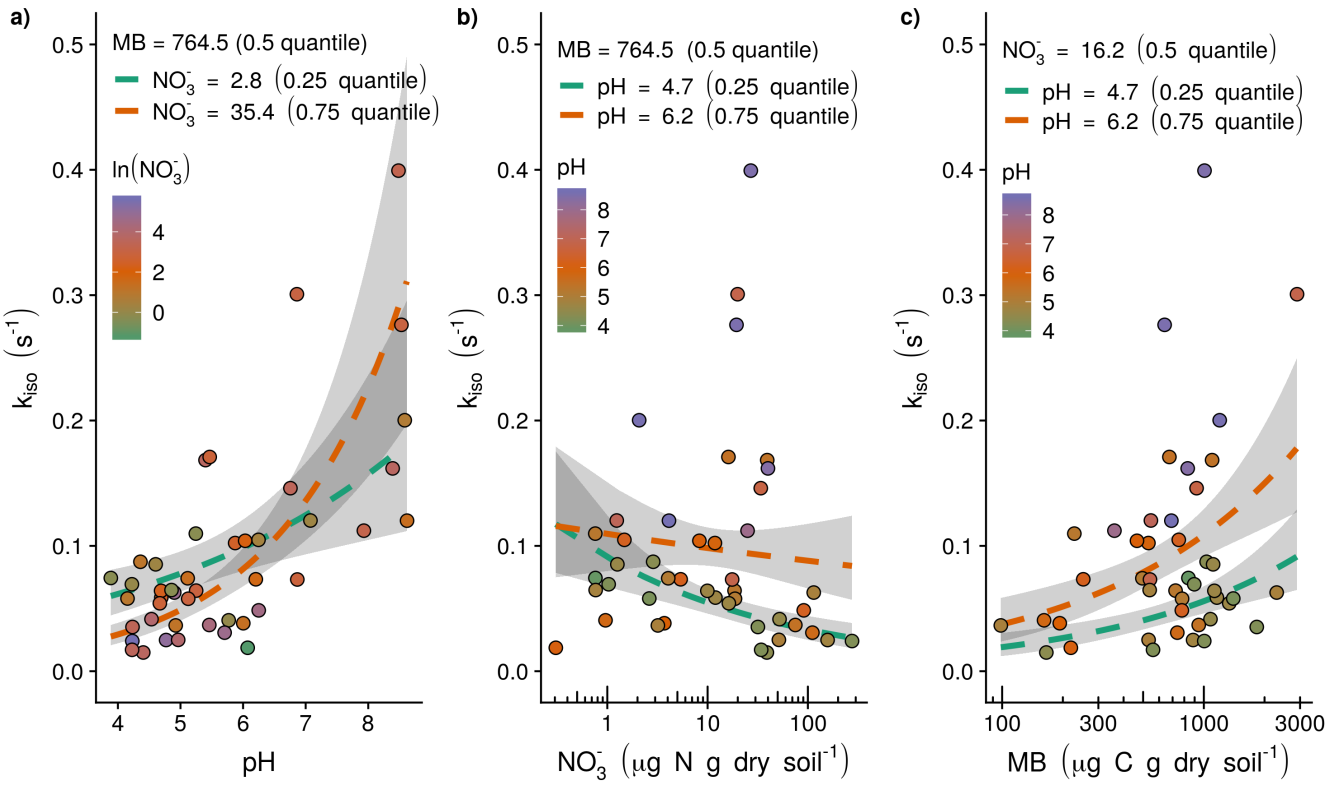

Figure 3: Observed (points) and modelled relationships following Eq. 6 (dashed lines) between the rate of oxygen isotope exchange (k_{iso}) and soil pH, NO_3^- availability and microbial biomass (MB): a) the positive relationship between k_{iso} and soil pH with model response as a function of the shown range in soil pH calculated with median microbial biomass and lower quartile (red dashed line) and upper quartile (blue dashed line) NO_3^- availability, b) the negative relationship between k_{iso} and NO_3^- availability with model response as a function of the shown range in NO_3^- availability calculated with median microbial biomass and lower quartile (red dashed line) and upper quartile (blue dashed line) soil pH, and c) the positive relationship between k_{iso} and microbial biomass with the model response as a function of the shown range in microbial biomass calculated with median soil pH and NO_3^- availability (red dashed line). Grey shaded areas indicate the 95 % confidence intervals associated with model fits.

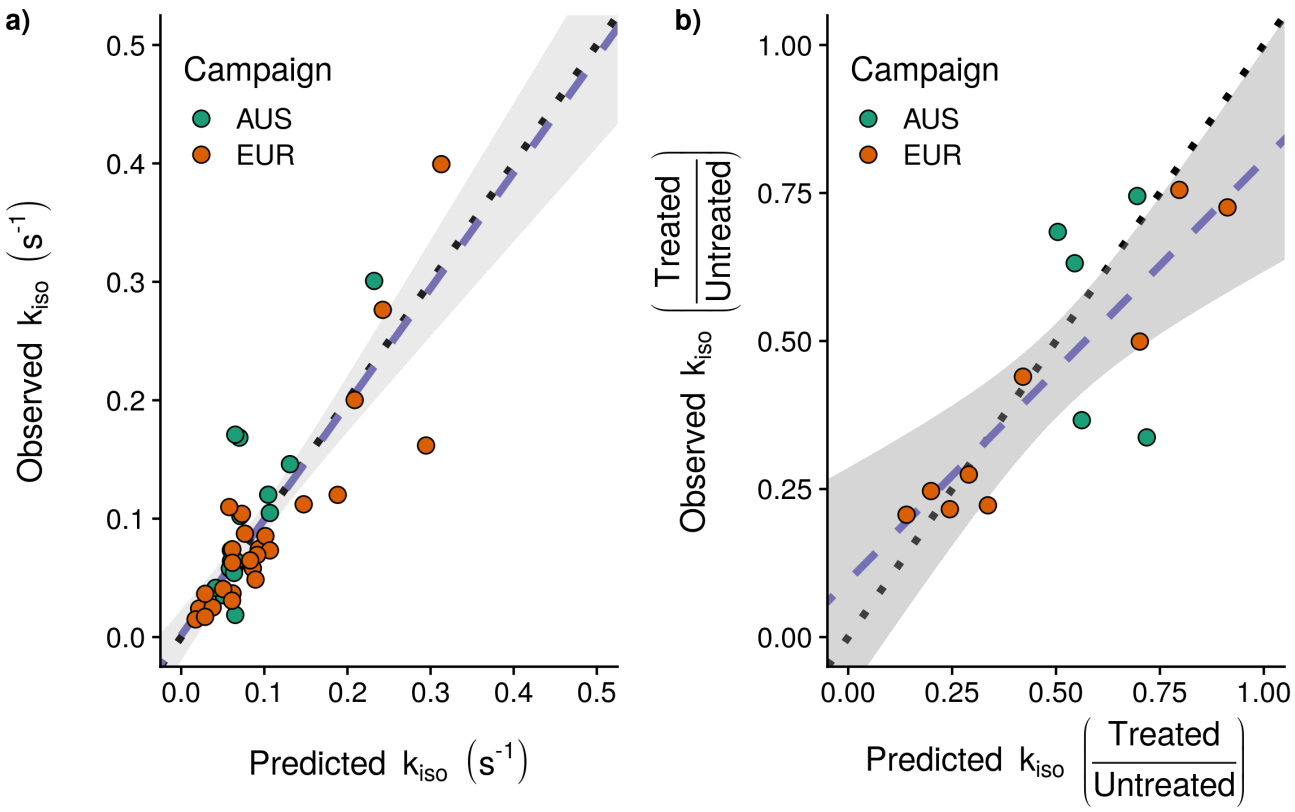

Figure 4: Rates of oxygen isotope exchange (k_{iso}) predicted by the minimal adequate model statistical model identified (Eq. 6): a) model predictions for the 44 untreated soils against the observations for these soils used in model fitting and b) predicted fractional changes in k_{iso} between treated and untreated soils against the changes observed following NH_4NO_3 addition. Plotted points indicate individual sites with the associate sampling campaign indicated by colour (EUR: blue, n = 9; AUS: red, n = 5), dotted lines indicate the 1:1 line and dashed blue lines indicate linear relationships between predicted and observed values with a shaded 95 % confidence interval.

715

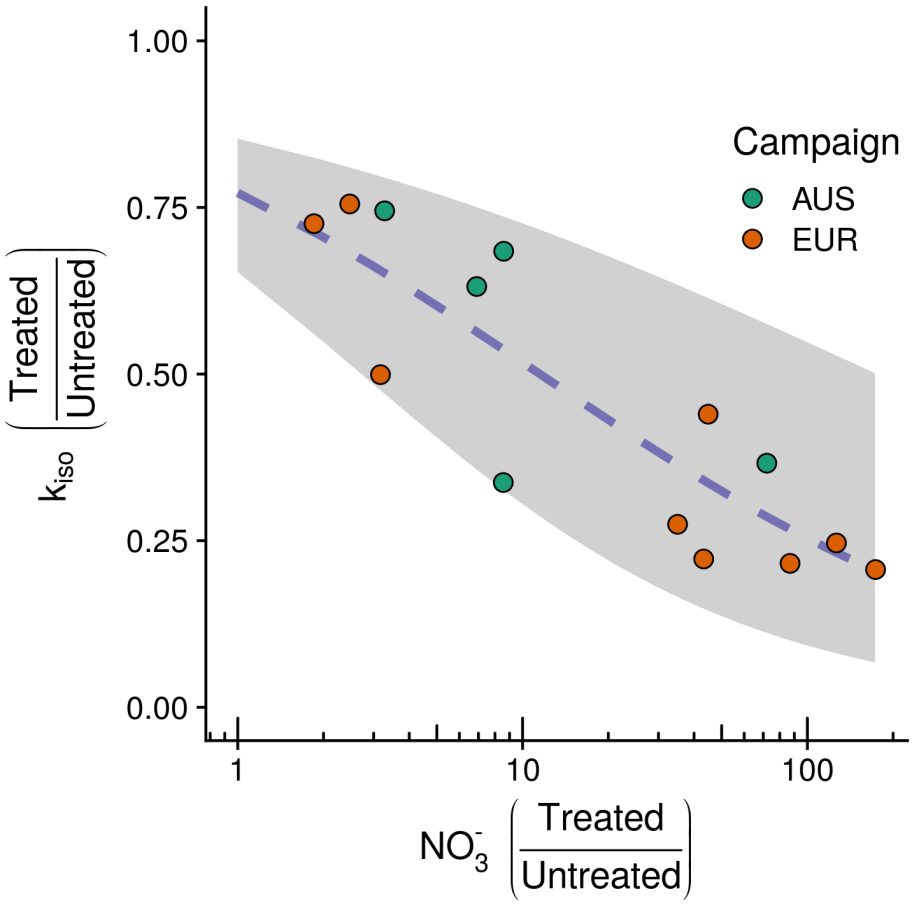

Figure 5: Observed negative relationship between the fractional change in the rate of oxygen isotope exchange (k_{iso}) and the fractional change in NO_3^- availability between treated and untreated soils following NH_4NO_3 addition for the 14 sites considered. Plotted points indicate the change for individual sites with the associate sampling campaign indicated by colour (EUR: blue, n= 9; AUS: red, n = 5). On the y-axis, quotients below 1 indicate k_{iso} in soils receiving the treatment decreased relative to corresponding untreated soils for each site. On the x-axis, quotients above 1 indicate NO_3^- availability in soils receiving the treatment increased relative to corresponding untreated soils for each site. The blue dashed line shows the fit of the minimal adequate generalised linear model describing the change in k_{iso} with 95 % confidence intervals shaded in grey.